Exploring the limits to energy scaling and distant-target delivery of high-intensity midinfrared pulses

Paris Panagiotopoulos,[1,2,*] Miroslav Kolesik,[1,2] and Jerome V. Moloney[1,2,3]
[1]*College of Optical Sciences, University of Arizona, Tucson 85721-0094, USA*
[2]*Arizona Center for Mathematical Sciences, University of Arizona, Tucson 85721-0094, USA*
[3]*Department of Mathematics, University of Arizona, Tucson 85721-0094, USA*
(Received 16 May 2016; published 28 September 2016)

We numerically investigate the scaling behavior of midinfrared filaments at extremely high input energies. It is shown that, given sufficient power, kilometer-scale, low-loss atmospheric filamentation is attainable by prechirping the pulse. Fully resolved four-dimensional ($xyzt$) simulations show that, while in a spatially imperfect beam the modulation instability can lead to multiple hot-spot formation, the individual filaments are still stabilized by the recently proposed mechanism that relies on the temporal walk-off of short-wavelength radiation.

DOI: 10.1103/PhysRevA.94.033852

I. INTRODUCTION

Worldwide efforts are actively under way to scale midinfrared (mid-IR) ultrashort laser pulses to supercritical powers capable of initiating and sustaining long-range filamentation in the atmosphere (the critical power scales as λ^2). Femtosecond-duration sources are anticipated to operate within the 3.5- to 4.1-μm atmospheric transparency window soon, delivering many tens to hundreds of millijoules. At even longer wavelengths, 9 to 11 μm, pulses with durations of hundreds of femtoseconds up to a few picoseconds are expected to deliver multiple-joule energies. The use of mid-IR wavelengths for atmospheric applications is important, since even ground-level turbulence is strongly mitigated at these longer wavelengths, as is well known for linear beams. As we see below a further advantage is that the nonlinear filament waists are typically much smaller than the inner scale of turbulence (scales as $\lambda^{6/5}$) at these longer wavelengths, further facilitating long-range propagation. Finally, the major limitation to the latter in this regime, namely, linear diffraction, is offset by filaments sustained over hundreds of meters and capable of transporting multiple terawatts of power.

Numerous theoretical and experimental works have recently investigated the properties of mid-IR filaments in gases. Bright coherent kilo-electron-volt x rays were generated in high-pressure capillaries through filamentation of $\lambda = 4$ μm pulses [1]. The extremely broad spectral bandwidth that can be generated by mid-IR pulses offers the possibility of generating zeptosecond-duration pulses, which was highlighted in Ref. [2]. The first experimental demonstration of a focused 3.9-μm, 200-GW filament in the atmosphere was demonstrated in [3]. Very recently it was shown that mid-IR pulses can be significantly compressed utilizing self-phase modulation followed by dispersion compensation [4], a well-established technique for ~800-nm wavelengths. Moreover, strong-field physics is also moving towards the utilization of mid-IR laser sources [5].

Previous theoretical work has demonstrated a new type of filamentation paradigm in the mid-IR, where the physics are driven by the electric field rather than the field envelope. Here nonlinearity, although weak, dominates over an even weaker dispersion in transparent solids and gases. The end result is the formation of a carrier wave shock well before the onset of critical self-focusing. This results in the generation of a cascade of spectrally broad dispersive waves encompassing multiple harmonics [6]. Moreover, filaments formed in this regime are about 10 times wider than their UV-to-near-IR counterparts, can transport much greater power and energy, and propagate over tens of meters with minimal ionization losses [7]. Extensive numerical studies showed that this new regime of low dispersion–high nonlinearity can indeed be found in various materials, such as noble gases and single-crystal diamonds [8].

Key observations from our current study are that mid-IR filamentation should be extremely robust and scalable to multiplekilometer ranges due primarily to cascades of carrier shock wave regularization events that limit the achievable peak intensities, thereby significantly reducing ionization losses typical of IR ultra-short pulses. While multiple filaments can form with very wide beams, their number is dramatically reduced, from hundreds with typical 100-μm waists to just a few with 1- to 2-mm waists due to a significant scaling-up of the underlying modulational instability growth wavelength.

II. NUMERICAL MODEL AND INPUT CONDITIONS

The numerical model used in the simulations is the unidirectional pulse propagation equation (UPPE). It is self-evident that optical carrier shocks, which prevail here, cannot be captured by a nonlinear envelope model. We initially adopt a radial symmetry to facilitate multiparameter studies. We later relax the radial symmetry assumption for two reasons: one is to account for symmtery-breaking multiple filamentation, and the second, less obvious reason is that artifical "rogue-wave-like" events observed in simulations downstream are often forced by such a symmetry restriction (see Supplementary Material to Ref. [7]). A detailed description of the numerical code can be found in [9].

The input wave packets used in this work have a central wavelength of 4 μm, with durations varying from 24 fs up to (chirped) 350 fs at full width half-maximum (FWHM) and beam waists that vary from 1.5 up to 9 cm at $1/e^2$ radius. The

*Corresponding author: parisps@email.arizona.edu

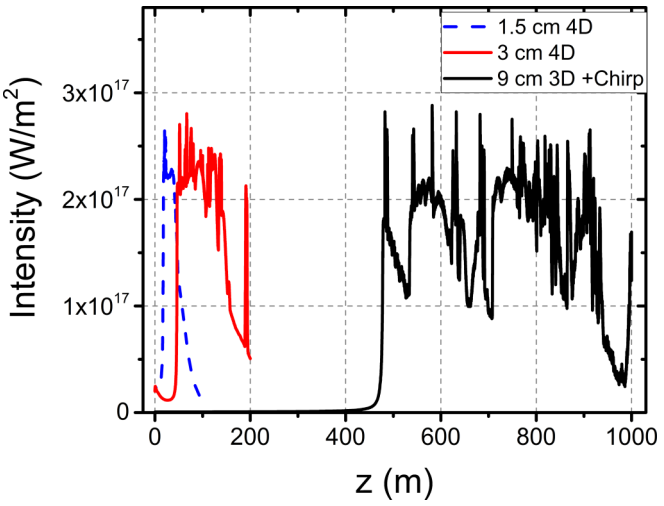

FIG. 1. Peak on-axis intensitys vs propagation distance for three different pulses. Dashed blue line: 24-fs, 1.5-cm input beam from [7]. Solid red line: 24-fs, 3-cm beam simulated under the assumption of axial symmetry over 200 m. Black line: 350-fs chirped pulse with a 9-cm beam waist simulated over a 1-km propagation distance (with the assumption of axial symmetry).

wave packets propagate in dry air at 1-atm pressure. Dispersion of air is modeled using the Sellmeier equation [10], while the nonlinear refractive index associated with self-focusing is extrapolated from 800 nm based on [11], and the ionization potential of oxygen is 12.03 eV, as was the case in [7].

III. RESULTS

In Fig. 1 we record the peak intensity of mid-IR filaments over a 1-km distance for three pulses propagating in dry air. The dashed blue line represents the 24-fs, 1.5-cm, 177-mJ wave packet studied in [3], forming a single filament roughly 40 m in length. The solid red line shows the scaling-up in input energy to 0.8 J, with the beam waist increased to 3 cm, in order to avoid strong Kerr self-focusing in the early stages of propagation. The filament is now well over 100 m long, being clamped to similar intensity values as in the lower energy case due to carrier shock walk-off, which keeps ionization losses to a minimum.

In order to extend mid-IR filamentation even further, we applied negative prechirp to the input wave packet. The resulting pulse is 350 fs long at FWHM, with a chirp parameter of $c = -10$. At low power the given pulse would fully time-compress down to 38 fs at a distance of roughly 1 km due to atmospheric dispersion. The temporal compression would increase the peak intensity by a factor of 9. This well-established technique has proven very effective in extending the length and delaying filament formation in the near-IR [12,13]. While prechirping delays the onset of filamentation, it was necessary to increase the beam waist to 9 cm, in order to keep the initial beam intensity low enough to prevent early self-focusing. Consequently, the input energy of this pulse is extremely high, at 2.87 J.

The peak intensity vs z of the chirped 350-fs, 9-cm wave packet is depicted in Fig. 1 as the solid black line. The filament forms abruptly at $z = 477$ m and persists over a 460-m distance, while maintaining a stable 1- to 2-mm beam waist after formation. The intensity profile is very similar to the lower energy cases, with multiple long-lasting plateaus and occasional spikes every ∼50 m. The temporal snapshots of the electric fields (not shown here) of both higher energy cases (red line, 0.8 J; black line, 2.87 J) show multiple walk-off events that extract energy out of the main pulse in the form of shock-seeded higher harmonics that propagate at a slower speed. This process is shown in a supplementary video of the radial-temporal intensity profile vs the propagation distance [14]. It shows the same mechanism found for the lower energy case (blue line, 177 mJ) recently studied in [7]. The overall energy losses over the 1-km propagation distance are ∼4%.

The spikes observed in the peak intensity every ∼50 m in the 2.87-J case are local on-axis hot spots that briefly overcome the walk-off mechanism only to be arrested by ionization and plasma defocusing. These on-axis spikes are accentuated in radial symmetric spatial computational grids (see Supplementary Material to Ref. [7]) and lead to an artificial enhancement in ionization losses relative to full four-dimensional (4D) simulations as we shall now show. In a previous work [7], we have shown that full 4D (xy: spatial dimensions, t, z) simulations can lead to notable differences compared to radially symmetric ones, especially for strongly perturbed input beams. Furthermore, by employing full 4D simulations we can investigate multifilamentation sourced by strongly aberrated initial beams. Notably, even the strong initial beam perturbations used in [7] did not result in a sustained modulation instability and multiple hot-spot formation. The main reasons behind the resilience of mid-IR filaments concerning beam breakup are the walk-off mechanism, the initially smaller transverse beam waist, and the scaling of the modulation instability growth as the inverse of the wavelength (see Supplementary Material to Ref. [7]).

In order to investigate mid-IR multiple filamentation in the atmosphere we simulated our highest energy case of chirped 350 fs, 9 cm, 2.87 J in four dimensions: two spatial dimensions, time, and propagation distance. To mimic a realistic wave packet we purposely added strong spatial random phase perturbations to the input beam profile in a similar fashion as in [7] (amplitude, 0.15; correlation length, 1 mm).

At this point we would like to note that simulating this 350 fs, 9 cm, 2.87 J wave packet in four dimensions with initial perturbations over a 1-km distance is an extremely demanding task. The simulation did run on our in-house SGI UV2000 supercomputer in parallel on 240 cores using ∼3 TB of shared RAM. The computation time was 2 calendar months. The computational box dimensions used were 20 cm×20 cm× 3 ps×1000 m with 2048×2048×4096 points, respectively, resolving a total of 16.1 billion degrees of freedom for a single-pulse snapshot and generating 2 TB of unprocessed data.

For all radial symmetric simulations shown in Fig. 1, numerical convergence was ensured by gradually increasing the resolution to the point where results remain unaffected. For the large 4D simulation described in the previous paragraph we use the highest resolution within our computational capabilities. While it was not possible to increase the resolution further, the given discretization does converge in radial symmetry. In addition, the simulation results show only a few minor

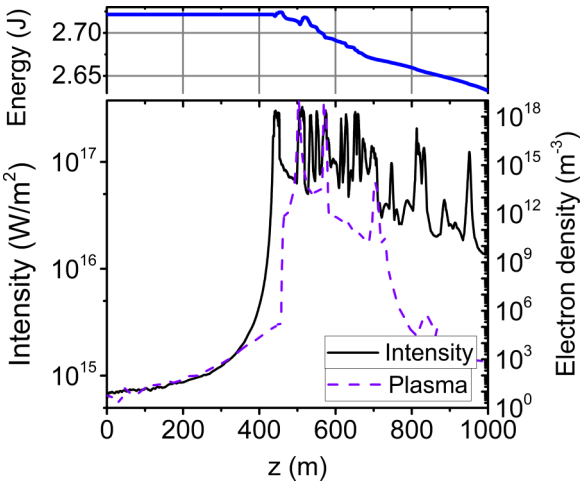

FIG. 2. Bottom: Peak intensity (solid black line) and integrated plasma density (dashed magenta line) vs propagation distance of a 350-fs chirped pulse with a 9-cm initial beam waist containing initial perturbations. Top: Total approximate energy contained in the computational box vs propagation distance. Simulation in *xyzt*.

numerical artifacts as shown in Figs. 2 and 3, as well as in the supplementary videos online [14]. The energy of the wave packet is calculated approximately by using a first-order integration scheme, which is less accurate than the simulation itself but sufficient for qualitative observation.

Figure 2 shows the peak intensity (solid black line), generated plasma density (dashed magenta line), and approximate total energy inside the computational box (blue line in the top inset) along the propagation distance. The filament is formed at $z \simeq 440$ m and is sustained with occasional spikes throughout the rest of the propagation. The generated plasma density is very low and only reaches values over 10^{18} m^{-3} twice, which keeps the energy losses as low as ∼3.26%, delivering more than 2.6 J at the 1-km distant target. Note that the bulk of the energy losses is due to the radiation leaving the computational box and being absorbed by the boundary (time, space, and spectral domains), while a small portion is lost due to ionization.

As in the radially symmetric case, the main regularizing mechanism here is higher harmonic walk-off, which continuously extracts energy out of the pulse in the temporal domain after the filament is formed. A video of the evolution of the on-axis electric field and on-axis spectrum along the propagation distance can be found in the Supplementary Material online [14]. As before, there are occasional instances where ionization occurs, here at $z \simeq 500$ m and $z \simeq 550$ m, when the walk-off mechanism cannot effectively offset self-focusing. While millijoule-level mid-IR filaments are mainly stabilized by higher harmonic walk-off, high-energy multijoule filaments, on the other hand, may involve infrequent ionization events when walk-off is not strong enough.

Figure 3 shows snapshots of transverse xy-fluence profiles at fixed distances along the propagation path corresponding to the data in Fig. 2. In the top left frame we can see xy fluence of the beam after propagating 100 m in the atmosphere, with the initial perturbations clearly noticeable. The remaining frames, from left to right, along the top show the formation of the two distinct hot spots, most pronounced at $z \simeq 460$ m. Note that the black square in the second graph indicates the zoomed-in axes used in the rest of the frames along the bottom row in Fig. 3, in order to show more detail. The dynamics get more complex from this point on, with the beam forming multiple hot spots at seemingly random locations. As expected the individual filament widths and lengths are consistent with those for lower energies, i.e., ∼1 mm wide and ∼30 m long. Unlike traditional 800-nm multifilaments, which generate multiple plasma channels, mid-IR multifilaments are extremely energy

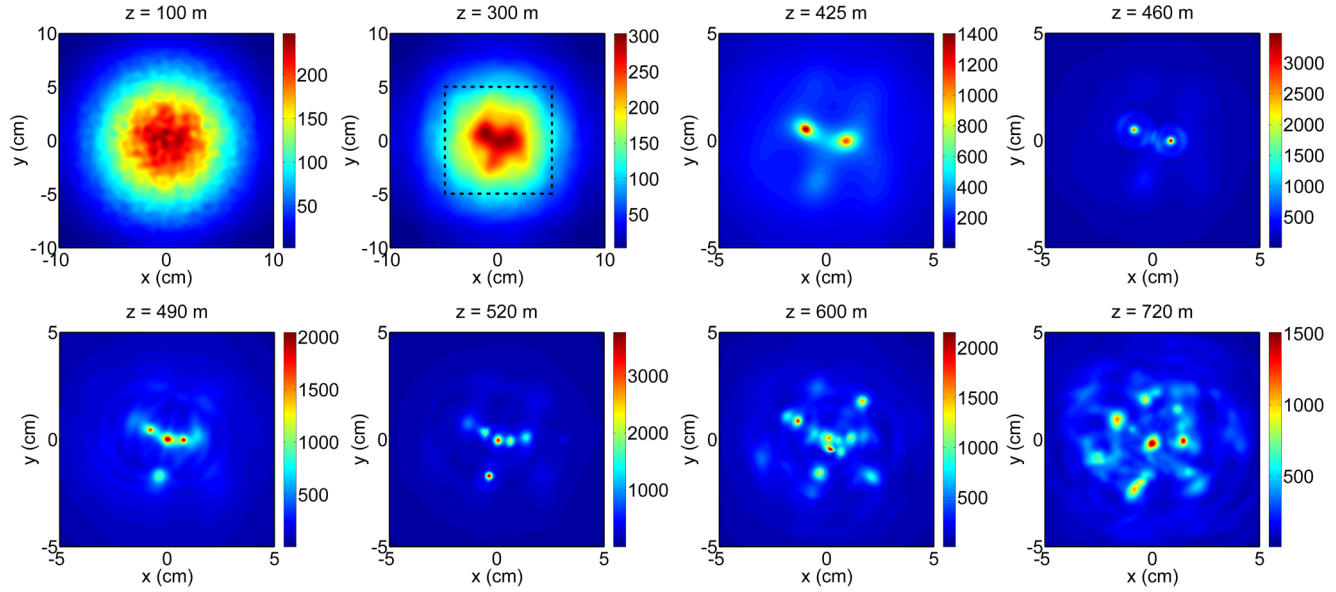

FIG. 3. Imperfect pulsed mid-IR beam breaking up in multiple filaments. *XY* cross section of fluence snapshots of the chirped 350-fs, 9-cm, 4-μm, 2.87-J wave packet with initial perturbations shown at various positions along the propagation distance. The dashed square in the second subfigure of first line indicates the region shown in the subsequent snapshots (10×10 cm). Simulation in *xyzt*. See supplementary video online [14].

efficient because of the very limited plasma generation, resulting in ∼4% of the total energy loss. A video showing the evolution of the xy fluence over the whole 1-km distance can be found in the Supplementary Material online [14].

IV. SUMMARY

In conclusion, we have investigated the filamentation of mid-IR pulses in the atmosphere and the scaling to high input energies. By negatively prechirping the input wave packet, we are able to predict that extremely long low-loss filaments can reach kilometer-long distances. We have shown that the walk-off mechanism responsible for the stabilization of lower energy mid-IR filaments is still the main regularization mechanism when energy is scaled up to the multijoule level. However, in extreme cases plasma generation does occasionally become necessary to arrest the collapse of the wave packet. While mid-IR beams can also break up into multiple filaments, individual filament characteristic waists at 4 μm remain at 1–2 mm and these are more robust due to slower modulational instability growth. We are currently aware of a large push to develop mid-IR ultrashort pulsed sources at tens to hundreds of millijoules at 4 μm and multijoule-level ultrashort pulses at 10 μm, making our results especially timely. We expect that properly engineered mid-IR filaments in the atmosphere will be scalable to even longer distances given enough power.

ACKNOWLEDGMENTS

This work was supported by the following research grants: Long Wavelength Electromagnetic Light Bullets Generated by a 10-μm CO_2 Ultrashort Pulsed Source (AFOSR FA9550-15-1-0272) and Carrier-Based Long-Wavelength Electromagnetic Light Bullets, Carrier Shock Initiated Exotic Waveforms and Extreme NLO Pulse Delivery to Targets (AFOSR FA9550-16-1-0088).

[1] C. Hernández-Garca, J. A. Pérez-Hernndez, T. Popmintchev, M. M. Murnane, H. C. Kapteyn, A. Jaron-Becker, A. Becker, and L. Plaja, Zeptosecond High Harmonic keV X-Ray Waveforms Driven by Midinfrared Laser Pulses, Phys. Rev. Lett. **111**, 033002 (2013).

[2] T. Popmintchev, M.-C. Chen, D. Popmintchev, P. Arpin, S. Brown, S. Aliauskas, G. Andriukaitis, T. Baliunas, O. D. Mcke, A. Pugzlys, A. Baltuka, B. Shim, S. E. Schrauth, A. Gaeta, C. Hernndez-Garca, L. Plaja, A. Becker, A. Jaron-Becker, M. M. Murnane, and H. C. Kapteyn, Bright coherent ultrahigh harmonics in the keV x-ray regime from mid-infrared femtosecond lasers, Science **336**, 1287 (2012).

[3] A. V. Mitrofanov, A. A. Voronin, D. A. Sidorov-Biryukov, A. Pugzlys, E. A. Stepanov, G. Andriukaitis, T. Flory, S. Alisauskas, A. B. Fedotov, A. Baltuska, and A. M. Zheltikov, Mid-infrared laser filaments in the atmosphere, Sci. Rep. **5** 8368 (2015).

[4] A. V. Mitrofanov, A. A. Voronin, D. A. Sidorov-Biryukov, S. I. Mitryukovsky, A. B. Fedotov, E. E. Serebryannikov, D. V. Meshchankin, V. Shumakova, S. Ali-auskas, A. Puglys, V. Y. Panchenko, A. Baltuka, and A. M. Zheltikov, Subterawatt few-cycle mid-infrared pulses from a single filament, Optica **3**, 299 (2016).

[5] B. Wolter, M. G. Pullen, M. Baudisch, M. Sclafani, M. Hemmer, A. Senftleben, C. D. Schroter, J. Ullrich, R. Moshammer, and J. Biegert, Strong-Field Physics with Mid-IR Fields, Phys. Rev. X **5**, 021034 (2015).

[6] P. Whalen, P. Panagiotopoulos, M. Kolesik, and J. V. Moloney, Extreme carrier shocking of intense long-wavelength pulses, Phys. Rev. A **89**, 023850 (2014).

[7] P. Panagiotopoulos, P. Whalen, M. Kolesik, and J. V. Moloney, Super high power mid-infrared femtosecond light bullet, Nat. Photon. **9**, 543 (2015).

[8] P. Panagiotopoulos, P. Whalen, M. Kolesik, and J. V. Moloney, Carrier field shock formation of long-wavelength femtosecond pulses in single-crystal diamond and air, J. Opt. Soc. Am. B **32**, 1718 (2015).

[9] M. Kolesik and J. V. Moloney, Nonlinear optical pulse propagation simulation: From Maxwell's to unidirectional equations, Phys. Rev. E **70**, 036604 (2004).

[10] E. R. Peck and K. Reeder, Dispersion of air, J. Opt. Soc. Am. **62**, 958 (1972).

[11] J. K. Wahlstrand, Y.-H. Cheng, and H. Milchberg, Absolute measurement of the transient optical nonlinearity in N_2, O_2, N_2O, and Ar, Phys. Rev. A **85**, 043820 (2012).

[12] H. Wille, M. Rodriguez, J. Kasparian, D. Mondelain, J. Yu, A. Mysyrowicz, R. Sauerbrey, J. P. Wolf, and L. Woste, Teramobile: A mobile femtosecond-terawatt laser and detection system, Eur. Phys. J. Appl. Phys. **20**, 183 (2002).

[13] P. Rairoux, H. Schillinger, S. Niedermeier, M. Rodriguez, F. Ronneberger, R. Sauerbrey, B. Stein, D. Waite, C. Wedekind, H. Wille, L. Wste, and C. Ziener, Remote sensing of the atmosphere using ultrashort laser pulses, Appl. Phys. B **71**, 573 (2000).

[14] See Supplemental Material at http://link.aps.org/supplemental/10.1103/PhysRevA.94.033852 for Movie 1km3DIrt, Movie 1km4DField, Movie 1km4DSpectrum, Movie 1km4DFluence.